Journal of Hydrology 566 (2018) 164–174

Contents lists available at ScienceDirect

Journal of Hydrology

journal homepage: www.elsevier.com/locate/jhydrol

Research papers

Potential ENSO effects on the oxygen isotope composition of modern speleothems: Observations from Jiguan Cave, central China

Zhe Sun[a,b,c], Yan Yang[a,*], Jingyao Zhao[d], Ning Tian[a], Xiangxiang Feng[a]

[a] Chongqing Key Laboratory of Karst Environment, School of Geographical Sciences, Southwest University, Chongqing 400715, China
[b] Key Laboratory of Tibetan Environment Changes and Land Surface Processes, Institute of Tibetan Plateau Research, Chinese Academy of Sciences, Beijing 100101, China
[c] University of Chinese Academy of Science, Beijing 100049, China
[d] Institute of Global Environmental Change, Xi'an Jiaotong University, Xi'an 710049, China

ARTICLE INFO

This manuscript was handled by Huaming Guo, Editor-in-Chief, with the assistance of Pedro J. J Depetris, Associate Editor

Keywords:
Oxygen isotope
Precipitation
Karst drip water
Modern speleothems
El Niño Southern Oscillation
Jiguan Cave
Central China

ABSTRACT

Despite of the fast development of speleothem records, oxygen isotope ($\delta^{18}O$), the main paleoclimatic proxy, remains complicated in climatic interpretation. Continuous cave monitoring is essential for understanding the response of stalagmite oxygen isotope to East Asian Summer Monsoon moisture transportation. We introduce a 7 years (2010–2016) study on oxygen isotope of atmospheric precipitation, cave drips and modern speleothems at Jiguan Cave, central China, located Chinese north–south divide where is sensitive to Asian Monsoon. The monitoring covered a whole ENSO (El Niño Southern Oscillation) cycle, from El Niño in 2010 to La Niña in 2011 and recovered another El Niño in 2015. The precipitation $\delta^{18}O$ shows obvious seasonality (negative in summer and positive in winter), but air temperature and rainfall amount are not primary controlling factors. The interannual $\delta^{18}O$ of precipitation corresponds with ENSO variability, which means $\delta^{18}O$ value is positive during El Niño event and vice versa. We used HYSPLIT (Hybrid Single Particle Lagrangian Integrated Trajectory) model to simulate the moisture transportation for rainy season in El Niño and La Niña years, and found the Pacific contributed over 50% moisture in El Niño years and the Indian Ocean was the predominant oceanic source in La Niña year. There is no seasonality in drips $\delta^{18}O$ value, while the response to ENSO variability is evident on interannual scale. The stable negative $\delta^{18}O$ of drips compared with precipitation indicate there is a threshold for infiltration, suggesting cave drips are recharged by summer heavy precipitation with light $\delta^{18}O$ value, but it's the mixture of latest and former rainy precipitation that recharge drips in drought, which has been verified by simple infiltration model. We found the modern speleothems were precipitated under nonequilibrium fractionation during drought years, nevertheless, they can record the El Niño related $\delta^{18}O$ positive anomaly. Overall, the modern speleothems can receive the precipitation $\delta^{18}O$ signal transferred by drips, and our study offers significance for verification of Asian Summer Monsoon driving force and interpretation of stalagmite $\delta^{18}O$.

1. Introduction

Stalagmite, the vital archive for paleoclimate reconstruction, has developed fast recently due to its series of advantages, such as precise dating, widely distribution, continuous precipitation, copious proxies and little external disturbance (e.g., Banner et al., 2007; Cai et al., 2008, 2010; Cheng et al., 2009, 2016; Shopov et al., 2004; Tan et al., 2015; Wang et al., 2001, 2017; Yuan et al., 2004; Zhu et al., 2017). Nevertheless, as the most important proxy, the interpretation of $\delta^{18}O$ remains in argument. Previous studies attributed its controlling factors to rainfall amount or air temperature. For example, Fleitmann et al. (2004) found there was significant anticorrelation between stalagmite $\delta^{18}O$ and bands thickness, which reflected the precipitation variation. Bar-Matthews et al. (2003) revealed the most negative in stalagmite $\delta^{18}O$ from north and central Israel was synchronic with the heaviest rainfall in east Mediterranean. The air temperature was introduced to explain the stalagmite $\delta^{18}O$ variation in Ireland and Austria (e.g., Mangini et al., 2005; McDermott et al., 1999), and supported by the contemporary increasing growth rate.

In general, the stalagmite $\delta^{18}O$ is usually regarded as the East Asian Monsoon signal in China (e.g., Cai et al., 2010; Cheng et al., 2009; Dayem et al., 2010; Hu et al., 2008; Maher, 2008; Yuan et al., 2004). Wang et al. (2001) suggested it was controlled by the ratio between summer and winter precipitation, and Hu et al. (2008) emphasized the

* Corresponding author at: No. 2 Tiansheng Road, Beibei District, Chongqing 400715, China.
E-mail addresses: michael2482004@126.com (Z. Sun), yy2954@swu.edu.cn (Y. Yang), zjyunicorn@stu.xjtu.edu.cn (J. Zhao), 2840142455@qq.com (N. Tian), 827453214@qq.com (X. Feng).

https://doi.org/10.1016/j.jhydrol.2018.09.015
Received 27 February 2018; Received in revised form 1 August 2018; Accepted 8 September 2018
Available online 10 September 2018
0022-1694/ © 2018 Elsevier B.V. All rights reserved.

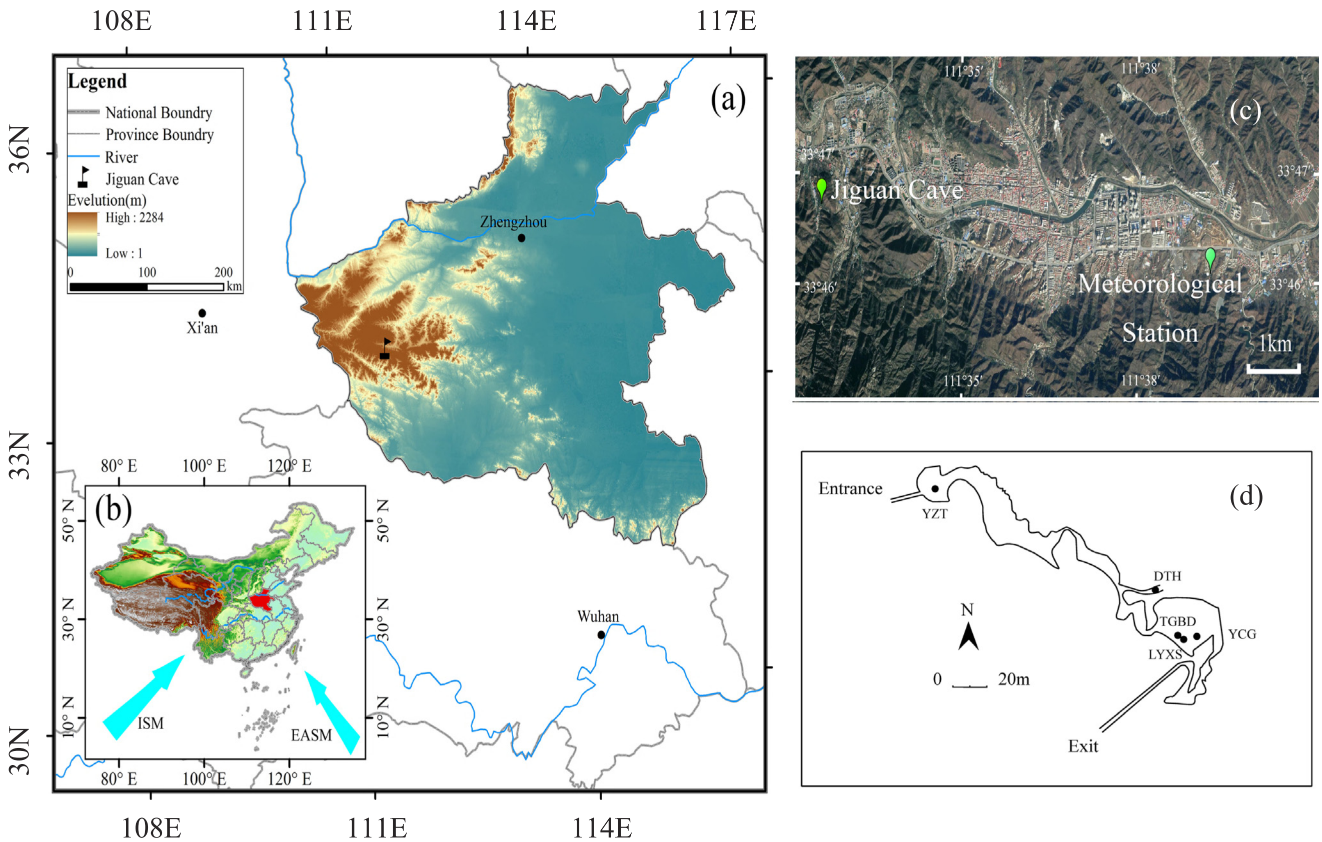

Fig. 1. (a) Location of study site, flag is Jiguan Cave and black dots are the cities included in GNIP (global network of isotopes in precipitation) and referenced in this article, (b) the background of study area and two main monsoon systems influencing this region (ISM: Indian Summer Monsoon, EASM: East Asian Summer Monsoon). (c) Google earth map of Luanchuan County. Jiguan Cave and meteorological station, indicated by green marks. (d) Schematic map of Jiguan Cave. The sampling sites are marked by black dots. YZT (Yu Zhu Tan) and YCG (Yao Chi Gong) are pools, LYXS (Li Yu Xi Shui) and TGBD (Tian Gong Bing Deng) are drips, DTH (Dong Tian He) is underground river in the cave. (For interpretation of the references to colour in this figure legend, the reader is referred to the web version of this article.)

rainfall amount effect. Some researches, however, preferred the change of moisture source rather than amount effect during Holocene in China (e.g., Maher, 2008; Maher and Thompson, 2012). Such conclusion is partly supported by Clemens et al. (2010) and Dayem et al. (2010) who suggested the change of moisture source and upstream rainout process should be taken into consideration.

Cave monitoring is an effective method to accurately understand the speleothem $\delta^{18}O$ significance, and such study has been implemented as early as 1980s (Yonge et al., 1985). Treble et al. (2005) disclosed the evident anticorrelation between precipitation $\delta^{18}O$ and rainfall amount at Moondyne Cave, SW Australia, likely indicating the inaccurate interpretation of stalagmite $\delta^{18}O$ as regulated by temperature. Given the evenly distributed rainfall throughout the year, the seasonality of precipitation $\delta^{18}O$ was attributed to the seasonal change in moisture source at Gunung Mulu and Gunung Buda National Park (Cobb et al., 2007). Furthermore, because of homogenization in the bedrock, cave drips generally exhibit more smooth $\delta^{18}O$ pattern than precipitation, suggesting mixture before infiltrating into cave (eg., Bar-Matthews et al., 2003; Genty et al., 2014; Mischel et al., 2015; Moerman et al., 2014; Vaks et al., 2003). Hence, the stable drips $\delta^{18}O$ are commonly regarded as the mean annual amount weighted precipitation $\delta^{18}O$ for local region (eg., Williams and Fowler, 2002; Yonge et al., 1985), but due to evaporation happened in epikarst or rapid infiltration, drips $\delta^{18}O$ can still reflect apparent variation (eg., Bar-Matthews et al., 1996; Cruz et al., 2005; Denniston et al., 1999; Van Rampelbergh et al., 2013).

Cave monitoring has been widely carried out in south China. The good correlation between $\delta^{18}O$ of precipitation and drips and meteorological parameters (air temperature and rainfall amount) suggests speleothem $\delta^{18}O$ records monsoon variation (Li et al., 2000). Li et al. (2011) found the drips $\delta^{18}O$ in Furong Cave showed stable value with no evident rate change, which was attributed to the mixture of atmospheric precipitation. The positive correlation between drip $\delta^{18}O$ and drip rate was observed at Liangfeng Cave (Luo et al., 2014). And the homogenization effect can be demonstrated by the decreasing $\delta^{18}O$ amplitude of precipitation, soil water and drips (Luo et al., 2013). Duan et al. (2016) compiled 8 long term monitoring caves in China, and found anti temperature effect was observed in 7 caves and the amount effect was feeble. The precipitation $\delta^{18}O$ cannot be simply contributed to temperature or amount effect because of various moisture sources.

As discussed above, current interpretation of speleothem $\delta^{18}O$ basically focuses on amount effect (eg., Bar-Matthews et al., 2003; Fleitmann et al., 2004; Hu et al., 2008), temperature effect (eg., Feng et al., 2014; Mangini et al., 2005), monsoon intensity (eg., Cheng et al., 2016; Wang et al., 2005; Yuan et al., 2004), and moisture source change (eg., Cobb et al., 2007; Dayem et al., 2010; Maher, 2008; Maher and Thompson, 2012). Actually, the parallel speleothem $\delta^{18}O$ variation in Chinese monsoon region on different time scales (Liu et al., 2015) potentially suggests controlled by same circulation pattern. Dayem et al. (2010) found the spatial distance of contemporary speleothems with parallel $\delta^{18}O$ variation was far than 500 km, which was the critical distance for areas share similar meteorological condition. To explain this phenomenon, Tan (2014, 2016) proposed circulation effect, which suggested West Pacific Subtropical High (WPSH) shifted more westwards during El Niño events, thus drove more proximal Pacific moisture to East Asia, and the shorter Rayleigh distillation distance made the ultimate precipitation with positive $\delta^{18}O$. During La Niña events, however, WPSH moved more eastwards, and moisture from distal Indian Ocean relatively increased. The longer distance depleted more ^{18}O, therefore resulted in more negative precipitation $\delta^{18}O$. Some monitoring and modeling studies have found the positive correlation between precipitation $\delta^{18}O$ and ENSO (El Niño Southern Oscillation) on interannual scale (e.g., Cai and Tian, 2016; Ishizaki et al., 2012; Vuille et al., 2005; Yang et al., 2016).

To testify the circulation effect, we choose Jiguan Cave, located southeast of Chinese Loess Plateau frontier where belongs to Chinese north–south divide and intersection of humid and semi-arid zone. Compared with high-latitude mainly influenced by temperature and the predominant amount effect in low-latitude, the special location of Jiguan Cave might be sensitive to different moisture sources. Moreover, this study started from 2010 to 2016, covering a whole ENSO cycle (El Niño in 2010&2015, La Niña in 2011). Through analyzing the $\delta^{18}O$ of precipitation, cave drips and modern speleothems, we offer significance for interpretation of speleothem and to verify the driving force for Asian Summer Monsoon.

2. Materials and method

2.1. Geographical setting and sample collection

Jiguan Cave (33°46′N, 111°34′E) is located at north slope of Funiu mountain (Fig. 1), ~4 km southwest of Luanchuan county, Henan Province, central China. The cave entrance altitude is ~900 m asl., the length is ~5600 m and one third has been developed for tourism. The average cave temperature is 16.4 °C and relative humidity keeps higher than 90% during monitoring period. Mean annual temperature and rainfall amount recorded by an adjacent meteorological station are 12.1 °C and 840.6 mm (1957–2014), respectively. More than 50% of annual precipitation occurs in rainy season (July-September). Some rainfall lasted more than one day, and some storm only lasted ~20 min. The host rock mainly consists of Cambrian limestone (Cai et al., 2008), with thickness ~30 to 40 m. Vegetation above the cave is dominated by conifers, oaks and bushes.

From 2010 to 2016, we almost collected every precipitation event. A precipitation event is defined by both the meteorological station and our precipitation collector. Sometimes, when the meteorological station reports rainfall but there is no water in our collector, it is not taken as an event, and vice versa. The meteorological station reports rainfall amount everyday (from 20:00 to 20:00), which is considered as an event and named using the date. Those rainfall events were named after the first day of raining if they lasted more than one day. In such case, we replaced new container at 20:00 to avoid enhanced evaporation. The multiple containers during such a long rainfall event were mixed and sealed using polyethylene vial and stored in fridge (approximately 4 °C) before measurement. Snow was sealed by same method after melt. The fast drip site (LYXS: Li Yu Xi Shui, consecutive drip with average rate ≈ 22 ml/min) and slow drip site (TGBD: Tian Gong Bing Deng, average rate ≈ 11 ml/min, hiatus in drought years) were collected in situ every 2 months, by the way, we also sampled 2 pools (YZT: Yu Zhu Tan and YCG: Yao Chi Gong) and an underground river (DTH: Dong Tian He) for parallel comparison. Modern speleothems were sampled by placing substrates under these 2 drips and substrate was also replaced every 2 months. Totally, we collected 284 precipitation, 182 cave water and 42 modern speleothem samples.

2.2. Isotope analysis

The oxygen and hydrogen isotopes of water samples were measured by water isotopes analyzer (IWA-35d-EP) of Los Gatos Research (LGR) Company. The standard reference is LGR3A/4A/5A from Los Gatos Research Company. As an analysis routine, LGR IWA analyzed each sample 6 times. Because residue of previous sample likely influences next sample (memory effect), the first two measurements were not taken as valid data. The 1σ precision (standard deviation based on sample measurement) is 0.2‰ for $\delta^{18}O$ and 0.6‰ for δD. The $\delta^{18}O$ and $\delta^{18}C$ of modern speleothems were measured using Finnigan Delta-V-Plus gas isotope mass spectrometer combined with Kiel IV automated carbonate device and specific details refer to Li et al. (2011). Each sample was analyzed 8 times, the long term 1σ precision (standard deviation based on sample measurement) is 0.1‰ for $\delta^{18}O$ and 0.06‰ for $\delta^{18}C$. Isotopic values are reported in delta notation relative to VSMOW (Vienna Standard Mean Ocean Water) for water and to VPDB (Vienna Pee Dee Belemnite) for modern speleothems.

2.3. Climate data and back trajectory model

The air temperature and precipitation amount were supplied by local meteorological station, located in the east county, ~8.4 km away from Jiguan Cave. NINO 3.4 SST anomaly data is downloaded from NOAA (National Oceanic and Atmospheric Administration) climate prediction center[18]. We used HYSPLIT Model (Stein et al., 2015) and Reanalysis daily data with 2.5° resolution to simulate and cluster air mass trajectories to affirm moisture source for every precipitation event in rainy season (July–September) during El Niño and La Niña years. Trajectories were performed four times every day (at UTC 00:00, 06:00, 12:00, and 18:00) and simulating height was set at 850 hPa and moved backward for 240 h (10 days). We choose 850 hPa because the moisture content in 850 hPa has been widely used as the main moisture transportation level in both Indian and East Asian monsoon regions, moreover, 850 hPa contains more moisture than other levels in central-north China (eg., Basha and Ratnam, 2013; Liang et al., 2013; Ma and Gao, 2006; Shen et al., 2010). All the statistic parameters involved in this manuscript were processed by SPSS19.

Table 1
Oxygen and hydrogen isotopes of precipitation, cave water and modern speleothems.

	min$\delta^{18}O$/‰ (VSMOW)	max$\delta^{18}O$/‰ (VSMOW)	Standard deviation/‰	minδD/‰ (VSMOW)	maxδD/‰ (VSMOW)	Standard deviation/‰	Sample number
Precipitation	-15.66	8.08	3.66	−118.29	45.81	29.24	284
LYXS (drip)	−10.20	−6.49	0.94	−70.10	−48.97	6.45	43
TGBD (drip)	−10.19	−6.43	1.39	−72.20	−49.43	8.42	10
YCG (pool)	−9.70	−5.58	0.96	−67.09	−39.13	7.43	43
YZT (pool)	−8.95	−3.73	1.40	−61.10	−35.13	6.47	43
DTH (underground river)	−9.24	−6.69	0.55	−63.60	−52.72	2.41	43
LYXS (carbonate)	−10.00	−5.02	1.37				27
TGBD (carbonate)	−10.09	−6.91	1.03				15

LYXS (Li Yu Xi Shui) and TGBD (Tian Gong Bing Deng) are acronyms of drips as scenic spots in Jiguan Cave; YCG (Yao Chi Gong) and YZT (Yu Zhu Tan) are acronyms of pools in the cave. DTH (Dong Tian He) is the acronym of underground river located in the deepest part of cave. VSMOW is Vienna Standard Mean Ocean Water.

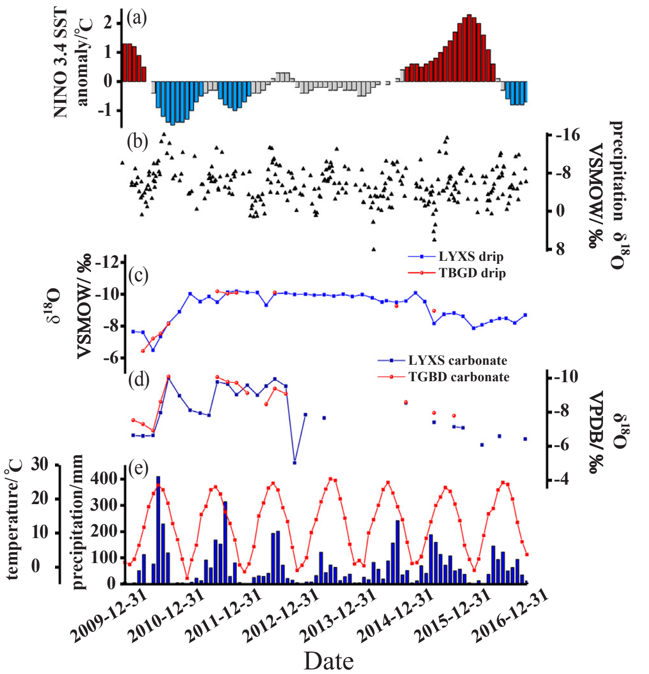

Fig. 2. Comparison between meteorological parameters, NINO3.4 sea surface temperature anomaly and oxygen isotopic composition of precipitation, drips and modern speleothems during monitoring period. All panels share same x-axis. (a: SST: sea surface temperature anomaly of NINO 3.4 region, red bars represent El Niño, grey bars represent normal condition and light blue bars represent La Niña, the raw data is offered by NOAA climate prediction center: http://origin.cpc.ncep.noaa.gov/products/analysis_monitoring/ensostuff/ONI_v4.shtml; b: oxygen isotopic composition of precipitation based on each precipitation event near Jiguan Cave; c: oxygen isotopic composition of drips. Blue dots represent LYXS, which is a fast consecutive dripping site and red dots represent TGBD, a slow dripping site located within the same hall; d: oxygen isotopic composition of modern speleothems collected under LYXS and TGBD. Blue dots represent LYXS and red dots represent TGBD; e: monthly mean air temperature and precipitation amount at Luanchuan county. Blue bars represent rainfall and red dots represent air temperature. Data are offered by local meteorological station, which is national base station.) (For interpretation of the references to colour in this figure legend, the reader is referred to the web version of this article.)

3. Result

3.1. Precipitation isotope

The variations of $\delta^{18}O$ and δD in precipitation are from −15.66‰ to 8.08‰ (average at −5.45 ± 3.66‰) and from −118.29‰ to 45.81‰ (average at −35.01 ± 29.24‰), respectively (Table 1). This isotopic variation is covered by previous Chinese precipitation isotopes report (Liu et al., 2014). The significant seasonality, positive in winter and negative in summer (Fig. 2b), has been introduced elsewhere in China (eg., Duan et al., 2016; Luo et al., 2013; Luo et al., 2014; Wang and LinHo, 2002; Wang et al., 2015; Xie et al., 2011). Some researchers contributed it to seasonal moisture source variation (eg., Araguas-Araguas et al., 1998; Duan et al., 2016; Feng et al., 2017; Hoffmann and Heimann, 1997; Thomas et al., 2016). For example, the monsoonal rainfall in summer generates lighter isotopes and inland or westerly moisture in winter, common in eastern and central China, leads to heavier isotopes.

3.2. Oxygen isotopes of cave water and modern speleothem

As showed in Fig. 3, the $\delta^{18}O$ of cave water fluctuated evidently, from −10.20‰ to −6.43‰ for drips, −9.70‰ to −3.73‰ for pools and −9.24‰ to −6.69‰ for underground. There is no seasonal variation in drips. Fast drip (LYXS) and slow drip (TGBD) rapidly reduced by 3.55‰ from 2009 to 2010 and kept stable (variation ≤ 0.88‰) in the following 4 years, then fast increased 2.23‰. The parallel pattern and approximate values suggest same recharge source. The deepest underground river (DTH) $\delta^{18}O$ showed similar pattern with more gentle variability. The changes of $\delta^{18}O$ in 2 pools are complex. YCG, the pool located nearby LYXS, showed deviating trend in comparison to LYXS despite it was recharged by LYXS, and YZT showed significant seasonality (negative in summer and positive in winter) since 2012.

The modern speleothems $\delta^{18}O$ values ranged from −10.00‰ to −5.02‰ (averaged at −8.02 ± 1.37‰) for LYXS and from −10.09‰ to −6.91‰ (averaged at −8.69 ± 1.03‰) for TGBD. It seemed modern speleothems $\delta^{18}O$ were seasonal in 2010 and 2011, negative in summer and positive in winter, which was similar to precipitation. Thereafter, LYXS showed stable negative value (−9.50‰ ± 0.34‰), and the synchronous drips exhibited comparable stability (−9.93‰ ± 0.33‰). Hiatus more than 1 year appeared since 2013 because of serious drought, and carbonate recovered in Nov. 2014 since drought was released by increasing rainfall and drips were oversaturated for precipitation (Sun et al., 2017). The $\delta^{18}O$ value was more positive than that of stable period by 2‰, which responded to the synchronous enrichment in precipitation and drips $\delta^{18}O$.

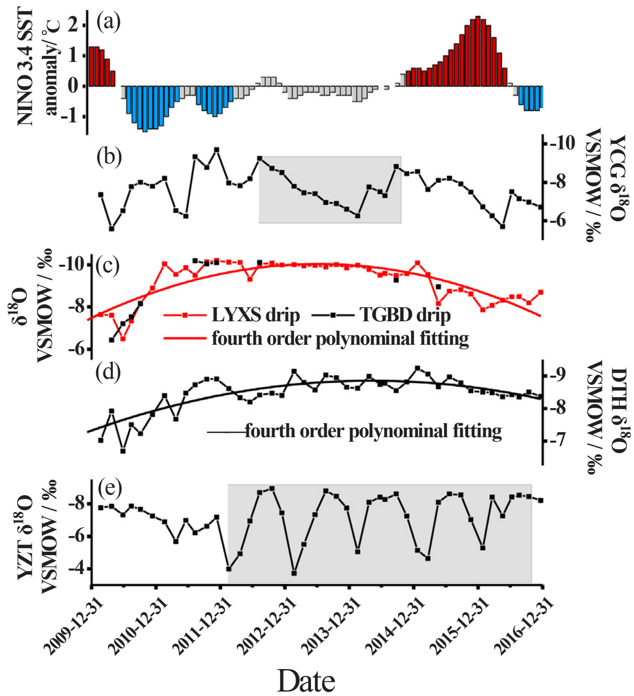

Fig. 3. Relationship between drips, pools and underground river $\delta^{18}O$ in Jiguan Cave (a: Sea Surface temperature anomaly of NINO 3.4 region, red bars represent El Niño, grey bars represent normal condition and light blue bars represent La Niña; b: $\delta^{18}O$ pattern of YCG; c: $\delta^{18}O$ pattern of LYXS and TGBD, red dots represent LYXS and black dots represent TGBD; d: $\delta^{18}O$ pattern of DTH; e: $\delta^{18}O$ pattern of YZT), the red and black curves are fourth order polynomial fitting results for LYXS and DTH, respectively. The grey shade in 3b represents extreme drought during monitoring and potential evaporation happened at YCG. The grey shade in 3e represents apparent seasonality of $\delta^{18}O$ since 2012. (For interpretation of the references to colour in this figure legend, the reader is referred to the web version of this article.)

4. Discussion

4.1. Controls on $\delta^{18}O$ of precipitation

Temperature effect (e.g., Dansgaard, 1964; Rozanski et al., 1992)

Table 2
Correlation coefficients between monthly weighted precipitation $\delta^{18}O$ and monthly mean air temperature and precipitation amount in study area.

r^2	$\delta^{18}O$	precipitation amount	air temperature
$\delta^{18}O$	1	0.036*	0.033
Precipitation amount		1	0.319***
air temperature			1

* Represent significance level is over 90% (2-tailed test).
*** Represent significance level is over 99.9% (2-tailed test).

and amount effect (e.g., Dansgaard, 1964; Jones and Banner, 2003) are denied because of poor correlation between monthly precipitation amount weighted $\delta^{18}O$ and meteorological data (shown in Table 2). Given the fact that there is a good correlation between air temperature and rainfall amount ($r^2 = 0.319$, $p < 0.001$, $n = 79$), and this phenomenon has been reported by other cave monitoring in Chinese monsoon region (eg., Ban et al., 2008; Duan et al., 2012; Li et al., 2011; Luo and Wang, 2008; Ruan and Hu, 2010), which means their relationships with precipitation $\delta^{18}O$ would be disturbed by each other. We also calculated PCC (partial correlation coefficient) to eliminate potential disturbance (e.g., Dayem et al., 2010; Johnson and Ingram, 2004). The PCC values are −0.109 ($p = 0.342$, $n = 79$) for $\delta^{18}O$ and amount and −0.091 ($p = 0.43$, $n = 79$) for $\delta^{18}O$ and temperature. The low correlation coefficients and PCC suggest temperature and precipitation amount are not predominant controlling factors for precipitation $\delta^{18}O$.

The good linear relationship between $\delta^{18}O$ and δD in precipitation was defined by Craig (1961) as GMWL (global meteoric water line): $\delta D = 8\ \delta^{18}O + 10$, and the study of meteoric water line is useful to understand climatic change and moisture source shift (Price et al., 2008). Gourcy et al. (2005) offered an updated GMWL: $\delta D = 8.07\ (\pm 0.02)\ \delta^{18}O + 9.9\ (\pm 0.1)$ by compiling all GNIP (global network of isotopes in precipitation) stations data from 1961 to 2000. The Chinese local meteoric water line (LMWL) was determined by Zheng et al. (1983): $\delta D = 7.9\ \delta^{18}O + 8.2$. Wei and Lin (1994) demonstrated that LMWL could vary on interannual scale among Chinese monsoon regions because of change in moisture source. We calculated the LMWLs every year at Luanchuan county (shown in Table 3). It is clear that the slope and intercept of LMWL in 2010 are evidently larger than that of GMWL, the slope and intercept of 2011 and 2013 are close to GMWL, and slope and intercept of 2012, 2014, 2015 and 2016 are obviously smaller than that of GMWL. We recalculated the LMWL based on all 284 precipitation events in 7 years since single year was unrepresentative, and result was $\delta D = 7.63\ (\pm 0.14)\ \delta^{18}O + 6.55\ (\pm 0.94)$, most similar to 2012. Merlivat and Jouzel (1979) suggested LMWL was determined by air temperature, rainfall amount and moisture source. While 2011 and 2013, with most similar LMWL, show the most temperature difference in the monitoring, and annual rainfall amount in 2011 is more than twice of 2013. Moreover, the slope and intercept of 2015 is obviously smaller than that of 2011 despite of their approximate annual temperature and rainfall amount. All of abovementioned analysis infer temperature and rainfall amount are not controlling factors for relationship of $\delta^{18}O$ and δD in precipitation.

Table 4
Amount weighted mean $\delta^{18}O$ of precipitation in study area (VSMOW/‰).

	2010	2011	2012	2013	2014	2015	2016
Jan		−12.29	−7.84	−3.62	−5.47	−5.54	−6.42
Feb	−5.71	−3.73	−3.49	−6.95	−5.16	− −7.20	−1.97
Mar	−6.40	−11.47	−2.27	−7.48	−5.15	−3.45	−7.23
Apr	−3.18	−0.42	−2.24	−2.62	−1.30	−2.98	−5.69
May		−8.43	−2.16	−2.53	−2.67	−3.30	−4.30
Jun	−4.91	−7.45	−8.29	−6.93	−4.73	−9.89	−6.88
Jul	−7.84	−11.02	−11.02	−8.83	−7.00	−7.16	−10.80
Aug	−7.86	−6.34	−8.91	−8.45	−7.39	−7.78	−8.64
Sep	−12.39	−5.13	−9.32	−9.44	−9.88	−4.39	−4.93
Oct		−5.89	−2.77	−8.69	−6.78	−4.36	−10.50
Nov	−6.77	−5.34	−7.88	−7.60	−8.75	−8.33	−4.07
Dec	−7.28	−8.33	−5.25			−4.99	−8.44
annual	−7.62	−8.50	−8.28	−6.17	−6.97	−5.78	−7.03

Null represents that station recorded some small rainfall but we did not collect precipitation sample or when we got sample but station did not record rainfall.

The monthly and annual weighted average precipitation $\delta^{18}O$ were calculated based on each precipitation event (Table 4, null represents we did not collect precipitation sample or rainfall amount data from meteorological station was not available). There is obvious inter-annual variation in $\delta^{18}O$, from −7.62‰ in 2010 to −8.50‰ in 2011. After 2011, precipitation $\delta^{18}O$ gradually enriched and reached its most positive value at −5.78‰ in 2015. This pattern is similar to ENSO variability (El Niño in 2010, 2015 and La Niña in 2011). Furthermore, the ENSO also imprinted on the rainfall amount. Previous studies reported the great possibility of more precipitation in East Asia during El Niño decaying phase (eg., Ju and Slingo, 1995; Zheng and Zhu, 2015), and this hypothesis is verified by the stupendous precipitation in Jul. 2010 (> 400 mm, twice in comparison to history record). The El Niño event in 2015 is the most powerful in this century, correspondingly, the amount weighted $\delta^{18}O$ is the most positive in monitoring, approximately equal to average $\delta^{18}O$ in Wuhan. Moreover, amount weighted $\delta^{18}O$ in 2011 (La Niña event) is most negative and even lighter than precipitation $\delta^{18}O$ of Xi'an and Zhengzhou (IAEA/WMO, 2001). Given the positive correlation between amount weighted precipitation $\delta^{18}O$ and NINO 3.4 SST Anomaly ($r = 0.715$, $p < 0.1$, $n = 7$), ENSO variability is potentially an important reason for interannual variation of precipitation $\delta^{18}O$.

Circulation effect speculates WPSH would shift more westwards during El Niño events, and drive more proximal Pacific moisture experienced less ^{18}O depletion to East Asia, thus leading to more positive precipitation $\delta^{18}O$ (Tan, 2014). To verify this assumption, we used HYSPLIT model and monthly Reanalysis data (2.5° resolution) offered by NOAA to simulate moisture trajectories for every precipitation event during rainy season (July to September) in 2010, 2015 (El Niño year) and 2011 (La Niña year). We divided the moisture source into three parts: Indian Ocean, the Pacific and others composed of China South Sea, inland, westerly and arctic sources. We suggested the vapor traced back to Arabian Sea and Bay of Bengal was treated as Indian Ocean origin. China South Sea was surrounded by Philippines, Vietnam,

Table 3
Local meteoric water line in study area.

year	sample number	slope	intercept	air temperature/°C	precipitation/mm	r^2
2010	39	8.94 ± 0.34	17.89 ± 2.54	12.50	1009.7	0.95
2011	33	8.39 ± 0.53	9.82 ± 3.63	12.05	949.5	0.89
2012	42	7.64 ± 0.34	6.77 ± 2.18	12.17	639.8	0.92
2013	36	8.24 ± 0.46	9.10 ± 3.10	13.65	434.6	0.90
2014	39	6.92 ± 0.42	2.12 ± 2.43	12.91	782.5	0.88
2015	51	7.16 ± 0.29	5.81 ± 1.80	12.63	911.4	0.93
2016	44	7.34 ± 0.38	3.94 ± 2.43	13.31	673.0	0.90
2010 ~ 2016	284	7.63 ± 0.14	6.55 ± 0.94	12.71	771.5	0.91

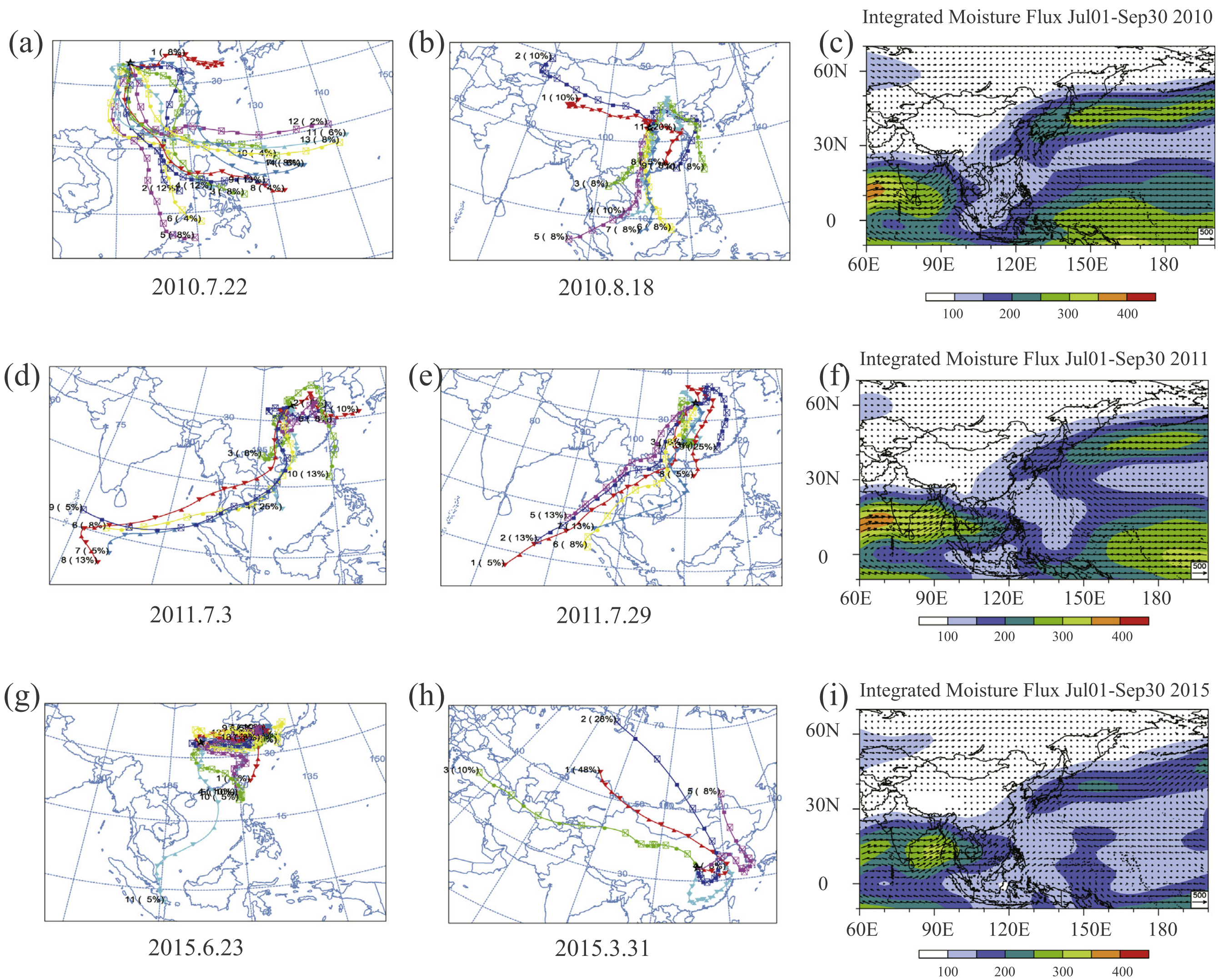

Fig. 4. Cluster analysis of backward trajectory for the top 2 heaviest precipitation event (a, b, d, e, g, h) and the integrated water vapor flux of rainy season in 2010& 2011&2015 (c, f, i, vector unit: kg/m/s), the original data is offered by NOAA Air Resources Laboratory (Reanalysis data: https://ready.arl.noaa.gov/ready2-bin/extract/extractfile.pl) and NCEP/NCAR Reanalysis Monthly Means (https://www.esrl.noaa.gov/psd/data/gridded/data.ncep.reanalysis.derived.surfaceflux.html).

Malaysia and China mainland. The Pacific source is defined as the vapor originated near east Chinese and Japanese coastlines. The other three sources, accounting for little significance, maily reflect vapor from local or westerly transportation and polar intrusion. As shown in Fig. 4 and Table 5, the Pacific predominately contributed 63% and 55% of moisture (amount weighted proportion) in 2010 and 2015, respectively. The Indian Ocean became the main marine moisture source in 2011, accounting for 38%, while the Pacific contributed to 11%. The cluster results of top 2 heaviest precipitation in 3 rainy seasons and integrated moisture flux verify circulation effect (Fig. 4). We also calculated the correlation of total 39 precipitation events and different moisture sources. The correlation coefficients are 0.351 ($p < 0.05$, $n = 39$) and -0.451 ($p < 0.01$, $n = 39$) for Pacific and Indian Ocean, respectively (Table 5). In fact, the monthly precipitation distribution in 2015 exhibited anomalies. The majority of precipitation occurred in advance from March to June. We simulated the strongest precipitation on 31st March (> 50 mm/d) and found most moisture originated from inland or transported by westerly (Fig. 4h). Pre-monsoon precipitation is enriched in ^{18}O (Yu et al., 2014). It might be this temporal anomalous precipitation combined with El Niño effect result the most positive oxygen isotope in 2015.

Although there are many reports have emphasized the effects of upstream process and convection intensity in vapor source on the interannual variation of precipitation oxygen isotope (eg., Cai and Tian, 2016; Cai et al., 2017; Lee and Fung, 2008; Liu et al., 2014; Moore et al., 2014), the above discussion indicates precipitation δ^{18}O is regulated by ENSO variability and the increasing proportion of moisture in Pacific is coming at the expense of Indian Ocean.

4.2. Relation of precipitation and drips

The inheritance of drips to precipitation after infiltration would be disturbed by specific cave system (Fairchild and Baker, 2012). The similar range and trend indicate LYXS and TGBD share same recharge source. There is no evident seasonal trend and CV (coefficient of variation) of LYXS is only 16.01% of precipitation. Such narrow amplitude has been reported by previous works (eg., Caballero et al., 1996; Genty et al., 2014; Li et al., 2011; Luo and Wang, 2008; Williams and Fowler, 2002; Yonge et al., 1985) and attributed to mixing process in overlying conduits and fissures. Generally, drips would be a reliable indicator for outside precipitation if there is no evident non-equilibrium fractionation during infiltration, the couple of δ^{18}O and δD would plot near the LMWL (e.g., Caballero et al., 1996; Cruz et al., 2005). And there is potential evaporation if drips plot below LMWL (Pape et al., 2010). The upper location of drips compared with LMWL infer no or less evaporation, furthermore, Clark and Fritz (1997) and Lacelle et al. (2004)

Table 5
Contribution of different moisture sources for precipitation event during rainy season (Jul–Sep) in 2010, 2015 (El Niño) and 2011 (La Niña).

Date	$\delta^{18}O$ (VSMOW/‰)	Precipitation/mm	Indian Ocean/%	The pacific/%	Other sources/%
2010-7-1	−6.41	9.7	15	63	22
2010-7-2	−9.96	20.7	18	82	0
2010-7-8	−5.02	2.7	28	30	42
2010-7-9	−6.18	37.2	21	5	74
2010–7-15	−9.97	84	0	100	0
2010-7-22	−7.27	241.7	0	85	15
2010-7-31	−10.54	0	43	57	0
2010-8-4	−8.29	1.6	34	26	40
2010-8-10	−11.22	12.1	33	8	59
2010-8-18	−7.65	199.1	16	41	43
2010-9-5	−11.96	99	0	50	50
2010-9-24	−15.66	13	0	26	74
2011-7-1	−6.23	0.3	13	33	54
2011-7-3	−12.32	111.7	39	18	43
2011-7-12	−7.16	10.3	28	0	72
2011-7-21	−4.38	3.9	0	68	32
2011-7-29	−10.22	97.2	51	0	49
2011-8-4	−6.47	36.7	23	0	77
2011-8-16	−4.75	0	30	70	0
2011-8-18	−6.16	25.8	41	33	26
2011-8-28	−7.18	0	0	35	65
2011-9-4	−4.99	0	0	46	54
2011-9-9	−5.55	2.8	0	38	62
2011-9-27	−5.06	17.5	0	0	100
2015-7-14	−4.23	26.3	0	100	0
2015-7-21	−4.21	25.1	0	100	0
2015-7-30	−14.49	20.7	25	0	75
2015-8-4	−12.18	29.2	73	0	27
2015-8-9	−4.86	4.8	40	28	32
2015-8-11	−15.40	6.2	42	58	0
2015-8-18	−5.91	22	0	100	0
2015-8-23	−2.41	16.9	0	53	47
2015-8-26	−7.17	0.6	0	51	49
2015-8-29	−6.73	27.3	0	20	80
2015-9-4	−7.20	13.4	0	35	65
2015-9-9	−3.49	24.2	0	74	26
2015-9-22	−2.74	3.6	0	73	27
2015-9-24	−5.31	5.3	0	100	0
2015-9-28	−2.14	6.4	0	78	22

The moisture source is basically divided in 3 sections, including Indian Ocean, the Pacific and other composed of China south sea, inland, westerly, and tiny arctic vapor.
Correlation coefficient between precipitation $\delta^{18}O$ and Indian Ocean ratio: −0.451, $p < 0.01$, n = 39.
Correlation coefficient between precipitation $\delta^{18}O$ and the Pacific ratio: 0.351, $p < 0.05$, n = 39.

attributed such pattern to the fact condensed water mixed into drips or drips basically reflected the precipitation originated from humid marine moisture (Rozanski et al., 1992). In the monitoring, most drips are plotted above or near LMWL (Fig. 5), indicating negligible evaporation and drips are mainly recharged by precipitation. The multiyear $\delta^{18}O$ are −9.14 ± 0.97‰, −8.54 ± 1.56‰ and −5.57 ± 3.69‰ for LYXS, TGBD and precipitation, respectively. The relative negative values in drips are contradictory to the enrichment caused by evaporation or reaction between bedrock and water stored in fissures and conduits. Given the stability of drips $\delta^{18}O$ (variation ≤ 0.88‰) from 2011 to 2014, we suggest there is a threshold (eg., Bar-Matthews et al., 1996; Fairchild and Baker, 2012; Genty et al., 2014; Jones and Banner, 2003; Pape et al., 2010; Tooth and Fairchild, 2003) of precipitation need to be exceeded to form effective replenishment, which means precipitation would be lost by evaporation, transpiration or runoff in the epikarst if precipitation is small (Genty et al., 2014). Although the amount effect is suitable because heavy precipitation usually experienced serious depletion in ^{18}O, it's not reasonable to utilize this hypothesis to explain our result due to the poor relation between amount and precipitation

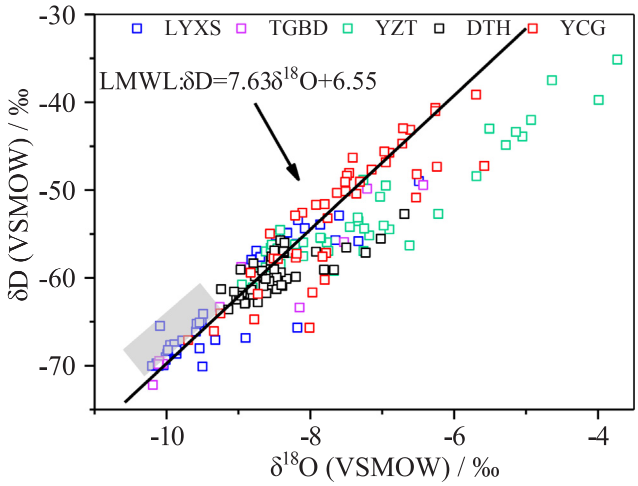

Fig. 5. Relationship between δD and $\delta^{18}O$ of cave water, shaded rectangle represents drips collected from LYXS during drought (2011–2014) with relative stable light $\delta^{18}O$ value, black line is the local meteoric water line.

$\delta^{18}O$ in our study area. The seasonal recharge might be why drips $\delta^{18}O$ are lighter than precipitation, since heavy monsoon rainfall (depleted in ^{18}O) occurred during July to September accounts for > 50% in the year. Therefore, rainy precipitation is the predominant recharge source. The plausible evidence is the drips from 2011 to 2014 plot above LMWL (shaded in Fig. 5), indicating humid marine origin (Rozanski et al., 1992), and the possibility of condensed water (eg., Clark and Fritz, 1997; Lacelle et al., 2004) is excluded due to fast dripping rate, which means the condensed water effect is of little importance. We chose the stable period (2011–2014) to verify our hypothesis because growing drought in this period was most likely to make rainy season the major recharge source. The method supplied by Moerman et al. (2014) was employed to calculate the amount weighted precipitation $\delta^{18}O$ in rainy seasons, corresponding drips $\delta^{18}O$ were set from current to next pre-rainy season weighted by dripping rate. The rainy precipitation $\delta^{18}O$ in 2010 was also calculated as we speculated it was the main replenishment for drips from rainy season in 2010 to pre-rainy season in 2011. Results showed $\delta^{18}O$ value of drips, from rainy season in 2010 to pre-rainy season in 2013, agreed well with the former latest rainy precipitation. While, drips exhibited ~0.6‰ to 1‰ lighter than rainy precipitation in 2013 and 2014 (Table 6). We suggest this deviation is caused by the serious drought, means the rainy precipitation is significantly less than usual and partly lost by evaporation in the soil. Therefore, the drips $\delta^{18}O$ reflect the combination of corresponding rainy precipitation and previous water in the overlying aquifer. We speculated the previous water is mixture of rainy precipitation from 2011 to 2012 or 2012, and utilized a simple bivariate model,

$$\delta^{18}O_d = \delta^{18}O_o \times f + \delta^{18}O_l \times (1-f)$$

where $\delta^{18}O_d$ is the isotopic composition of drip, $\delta^{18}O_o$ is the isotopic composition of previous water in aquifer, $\delta^{18}O_l$ is the isotopic composition of latest rainy precipitation, and f is the proportion of previous water in the mixture, to quantify different sources. The previous mixed precipitation from 2011 to 2012 and 2012 in aquifer are −9.79‰ and −9.88‰, respectively, hence, the rainy precipitation in 2013 contributed to only 3%–10%. The same method was implemented to verify rainy precipitation in 2014 and its following responding drips. We found the contribution of 2014 to drips increased to ~40%, which was corresponded to the rainfall recovery in the rainy season in 2014. Except for the stability during 2011–2014, drips in 2010 and 2015 showed most positive $\delta^{18}O$ value and largest amplitude (Fig. 3), corresponding to the active Pacific and negative Indian Ocean. Based on above discussion, the drips in Jiguan Cave mainly reflect the latest rainy precipitation or previous 1–2 years in ordinary and drought year,

Table 6
Comparison between $\delta^{18}O$ of rainy precipitation during 2010–2014 and following responding drips $\delta^{18}O$.

	2010 (VSMOW/‰)	2011 (VSMOW/‰)	2012 (VSMOW/‰)	2013 (VSMOW/‰)	2014 (VSMOW/‰)
Rainy precipitation	−8.55	−9.68	−9.88	−8.73	−8.53
Responding drip	−8.57	−9.82	−10.03	−9.76	−9.13

Precipitation is based on every event in rainy season (Jul.–Sep.) during 2010–2014 (stable and relative lighter $\delta^{18}O$ value) and responding drips $\delta^{18}O$ are weighted by dripping rate from current rainy season to next pre-rainy season. For example, −8.55‰ is the average precipitation $\delta^{18}O$ from Jul. to Sep. in 2010, and −8.57‰ is the average of LYXS from Jul.2010 to Jun.2011. TGBD is excluded for drip $\delta^{18}O$ calculation because of its long cutoff over 2 years in this period.

respectively. And the ENSO related variation of precipitation $\delta^{18}O$ can be recorded in drips on interannual scale.

The trend of DTH is similar to that of LYXS: the fast decrease (~2.22‰) from 2010 to 2011, relative stable period during 2011–2014, and gradually soared up since 2015. But the descent accomplished ~8 months later than drips and the amplitude was less than drips, which might be related to its deepest location, means longer mixture process. The $\delta^{18}O$ trend of YCG is complex, gentle decrease with fluctuation during 2010–2011 and gradual increase since 2014 seems similar to the drips and precipitation, while the unexpected increase from 2012 to 2014 punctuated this pattern. We suggest such deviation is the mirror of extreme drought during 2012–2014. Scenic staffs introduced some drips hiatus and the downside of DTH level, moreover, the relative humidity in 2013 decreased to ~90% allow for its usual value was > 95%. Given the long residence time exposed to air, the anomaly is basically cause by evaporation during drought, supported by the lower location compared with LMWL (Fig. 5). Another pool, YZT, showed distinct seasonal $\delta^{18}O$ cycle (negative in summer and positive in winter) since 2012. It is connected to entrance by manmade tunnel (~20 m) and the temperature pattern is same as outside. Therefore, temperature effect is not the reason for oxygen isotope variation. And it's not plausible to attribute seasonality to suddenly increase in conduits connectivity because of stable tectonic feature (Song et al., 2009). We suggest ventilation is the main cause since air exchange results condensed water in summer and evaporation in winter (De Freitas and Schmekal, 2003), this alternation explains seasonal oxygen isotopic cycle.

4.3. *Significance for modern speleothem*

It's crucial to verify whether speleothem was formed under equilibrium fractionation before paleoclimatic reconstruction (eg., Hendy, 1971; O'Neil et al., 1969). We chose Kim and O'Neil (1997):

$$\delta^{18}O_c - \delta^{18}O_w \approx 1000\ln\alpha(\text{calcite}-\text{drip}) = 18.03(10^3T^{-1}) - 32.42$$

hereinafter referred to as KO function, and Tremaine et al. (2011):

$$\delta^{18}O_c - \delta^{18}O_w \approx 1000\ln\alpha(\text{calcite}-\text{drip}) = 16.01(10^3T^{-1}) - 24.6$$

hereinafter referred to as T function, where $\delta^{18}O_c$ is the isotopic composition of modern speleothem (VPDB), $\delta^{18}O_w$ is the isotopic composition of drip (VSMOW), and T is Kelvin temperature, to verify our results (Fig. 6). It should be noted 2 months lag between drips and modern speleothems, for example, we suggest carbonate collected from June is corresponded to drips in April. There are little differences for simulated oxygen isotopic composition between 2 equations, ~1‰ heavier for T function. The mean $\delta^{18}O$ value of LYXS (−8.22 ± 1.38‰) is similar to T function (−8.26 ± 1.13‰) and mean $\delta^{18}O$ value of TGBD (−8.99 ± 1.00‰) is close to KO function (−9.02 ± 1.66‰). The difference of measured and simulated data is basically same with McDermott et al. (2011), however, the dramatic fluctuation in 2011–2014 (Fig. 2d) probably denote non-equilibrium fractionation. The intense positive deviation of $\delta^{18}O$ in Dec.2012 and Jun.2013 (~4‰, Fig. 6) responds to the serious drought in 2012 and 2013 reflected by positive anomaly in YCG $\delta^{18}O$ value, implying effect of evaporation.

There is an significant correlation between $\delta^{18}O$ and $\delta^{13}C$ in LYXS ($r = 0.556, p < 0.01, n = 27$), indicating nonequilibrium fractionation (Cai et al., 2010), and the correlation coefficient weakens to 0.497 (95% significance level) when we remove these anomalous positive data in drought years. The coefficient of TGBD is only 0.248 ($p > 0.1$, $n = 15$), which is corresponded to Mickler et al. (2004) conclusion that kinetic fractionation is easier to occur for drips with higher rate.

It's clear that $\delta^{18}O$ value of modern speleothem is controlled not only by drip, but also by the specific cave condition, such as dripping rate, temperature and relative humidity. Although the effect of drought results positive deviation, the oxygen isotopic composition of modern speleothem showed synchronous response to ENSO variation, positive in El Niño and negative in La Niña. Such phenomenon suggests that ENSO-driven precipitation $\delta^{18}O$ variation can be transferred to modern speleothem by drip. However, stalagmite should be prudently used for paleoclimate recovery when without cave monitoring research.

5. Conclusion

The results of 7 continuous years monitoring for precipitation, cave drips and modern speleothems are as follows: (1) the range of precipitation $\delta^{18}O$ is −15.66‰ to 8.08‰ and there is obvious seasonal variation, negative in summer and positive in winter. Statistic test suggests rainfall amount and air temperature are not basic controlling factors for precipitation $\delta^{18}O$ value. The interannual pattern responds to ENSO variability: heavier in El Niño and lighter in La Niña. The simulation of HYSPLIT model based on rainfall event in rainy season of ENSO years shows moisture from Pacific contributes more than 50% and Indian Ocean becomes the predominate marine source in El Niño and La Niña, respectively, which preliminarily verify circulation effect. (2) $\delta^{18}O$ of drips show narrow variation in comparison to precipitation and no seasonality because of homogenization in upper aquifer. The stable and light $\delta^{18}O$ value of drips in drought indicated that drips were recharged mainly by rainy season (July-September) precipitation with relatively negative $\delta^{18}O$ value because small rainfall might be lost by transpiration and evaporation in the overlying soil. Such hypothesis is verified by simple infiltration model, but it's the mixture of latest and previous rainy precipitation that replenish drips in drought. (3) We have carried out equilibrium fractionation test, and modern speleothems exhibit some nonequilibrium fractionation happened, especially during extreme drought period, ~4‰ more positive than simulated value. Nevertheless, the ENSO driven interannual pattern of precipitation $\delta^{18}O$ has been transferred to speleothems through drips.

Overall, it is of significance to emphasize the cave monitoring to further understand $\delta^{18}O$ process from precipitation to modern speleothem before climatic reconstruction.

Acknowledgements

We thank Prof. Tingyong Li in the Chongqing Key Laboratory of Karst Environment, Southwest University, China, and Prof. Juzhi Hou in Key Laboratory of Alpine Ecology and Biodiversity (LAEB), Institute of Tibetan Plateau Research, Chinese Academy of Sciences for assistance in the isotope analysis and useful discussion. This work was supported by grants of the National Natural Science Foundation of

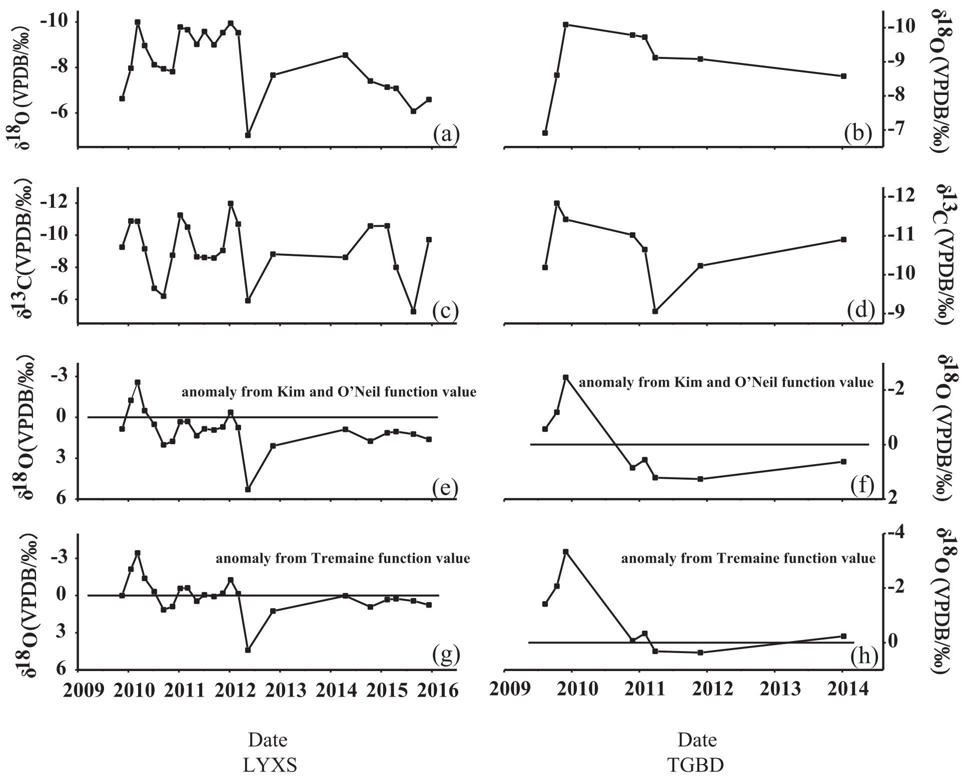

Fig. 6. Comparison between the $\delta^{13}C$, $\delta^{18}O$ of modern calcite and simulation under equilibrium fractionation condition (a&b: measured calcite $\delta^{18}O$ of LYXS and TGBD, c&d: measured calcite $\delta^{13}C$ of LYXS and TGBD, e&f: differences in $\delta^{18}O$ between measured LYXS and TGBD calcite and calibration from Kim and O'Neil (1997) function, g&h: differences in $\delta^{18}O$ between LYXS and TGBD calcite and calibration from Tremaine et al. (2011) function. All panels share same x-axis.).

China (41672160, 41372177 and 40902053), the National Key R&D Program of China (2016YFC050230205), the Research Fund for the Doctoral Program of Higher Education of China (20090182120005) and the Fundamental Research Funds for the Central Universities (XDJK2011B004).

References

Araguas-Araguas, L., Froehlich, K., Rozanski, K., 1998. Stable isotope composition of precipitation over southeast Asia. J. Geophys. Res. 103 (D22), 28721–28742. https://doi.org/10.1029/98jd02582.

Ban, F., et al., 2008. Temporal and spatial variations in the discharge and dissolved organic carbon of drip waters in Beijing Shihua Cave, China. Hydrol. Processes 22 (18), 3749–3758. https://doi.org/10.1002/hyp.6979.

Banner, J.L., et al., 2007. Seasonal variations in modern speleothem calcite growth in Central Texas, USA. J. Sediment. .earch 77 (7–8), 615–622. https://doi.org/10.2110/jsr.2007.065.

Bar-Matthews, M., et al., 2003. Sea–land oxygen isotopic relationships from planktonic foraminifera and speleothems in the Eastern Mediterranean region and their implication for paleorainfall during interglacial intervals. Geochim. Cosmochim. Acta 67 (17), 3181–3199. https://doi.org/10.1016/s0016-7037(02)01031-1.

Bar-Matthews, M., et al., 1996. Carbon and oxygen isotope study of the active water-carbonate system in a karstic Mediterranean cave: Implications for paleoclimate research in semiarid regions. Geochim. Cosmochim. Acta 60 (2), 337–347. https://doi.org/10.1016/0016-7037(95)00395-9.

Basha, G., Ratnam, M.V., 2013. Moisture variability over Indian monsoon regions observed using high resolution radiosonde measurements. Atmos. Res. 132–133 (10), 35–45.

Caballero, E., Cisneros, C.J.D., Reyes, E., 1996. A stable isotope study of cave seepage waters. Appl. Geochem. 11 (4), 581–585.

Cai, B., et al., 2008. A dry episode during the Younger Dryas and centennial-scale weak monsoon events during the early Holocene: a high-resolution stalagmite record from southeast of the Loess Plateau, China. Geophys. Res. Lett. 35. https://doi.org/10.1029/2007gl030986.

Cai, Y., et al., 2010. The variation of summer monsoon precipitation in central China since the last deglaciation. Earth Planet. Sci. Lett. 291 (1–4), 21–31. https://doi.org/10.1016/j.epsl.2009.12.039.

Cai, Z., Tian, L., 2016. Atmospheric controls on seasonal and interannual variations in the precipitation isotope in the East Asian Monsoon Region. J. Clim. 29 (4), 1339–1352. https://doi.org/10.1175/jcli-d-15-0363.1.

Cai, Z., Tian, L., Bowen, G.J., 2017. ENSO variability reflected in precipitation oxygen isotopes across the Asian Summer Monsoon region. Earth Planet. Sci. Lett. 475, 25–33. https://doi.org/10.1016/j.epsl.2017.06.035.

Cheng, H., et al., 2009. Ice Age Terminations. Science 326 (5950), 248–252. https://doi.org/10.1126/science.1177840.

Cheng, H., et al., 2016. The Asian monsoon over the past 640,000 years and ice age terminations. Nature 534 (7609), 640–646. https://doi.org/10.1038/nature18591.

Clark, I.D., Fritz, P., 1997. Environmental Isotopes in Hydrogeology. CRC Press.

Clemens, S.C., Prell, W.L., Sun, Y., 2010. Orbital-scale timing and mechanisms driving Late Pleistocene Indo-Asian summer monsoons: Reinterpreting cave speleothem δ18O. Paleoceanography 25 (PA4207), 545–558.

Cobb, K.M., et al., 2007. Regional-scale climate influences on temporal variations of rainwater and cave dripwater oxygen isotopes in northern Borneo. Earth Planet. Sci. Lett. 263 (3–4), 207–220. https://doi.org/10.1016/j.epsl.2007.08.024.

Craig, H., 1961. Isotopic variations in meteoric waters. Science 133 (346), 1702–1703. https://doi.org/10.1126/science.133.3465.1702.

Cruz, F.W., et al., 2005. Stable isotope study of cave percolation waters in subtropical Brazil: Implications for paleoclimate inferences from speleothems. Chem. Geol. 220 (3–4), 245–262. https://doi.org/10.1016/j.chemgeo.2005.04.001.

Dansgaard, W., 1964. Stable isotopes in precipitation. Tellus 16 (4), 436–468.

Dayem, K.E., et al., 2010. Lessons learned from oxygen isotopes in modern precipitation applied to interpretation of speleothem records of paleoclimate from eastern Asia. Earth Planet. Sci. Lett. 295 (1–2), 219–230. https://doi.org/10.1016/j.epsl.2010.04.003.

De Freitas, C.R., Schmekal, A., 2003. Condensation as a microclimate process: measurement, numerical simulation and prediction in the Glowworm Cave, New Zealand. Int. J. Climatol. 23 (5), 557–575. https://doi.org/10.1002/joc.898.

Denniston, R.F., et al., 1999. Evidence for increased cool season moisture during the middle Holocene. Geology 27 (9), 815–818. https://doi.org/10.1130/0091-7613(1999) 027<0815:eficsm>2.3.co;2.

Duan, W., et al., 2012. The growth mechanism of the aragonitic stalagmite laminae from Yunnan Xianren Cave, SW China revealed by cave monitoring. Boreas 41 (1), 113–123. https://doi.org/10.1111/j.1502-3885.2011.00226.x.

Duan, W., et al., 2016. The transfer of seasonal isotopic variability between precipitation and drip water at eight caves in the monsoon regions of China. Geochim. Cosmochim. Acta 183, 250–266. https://doi.org/10.1016/j.gca.2016.03.037.

Fairchild, I.J., Baker, A., 2012. Speleothem Science: From Process to Past Environments. Wiley-Blackwell.

Feng, F., et al., 2017. Stable isotopes in precipitation and atmospheric moisture of Pailugou Catchment in northwestern China's Qilian Mountains. Chin. Geogr. Sci. 27 (1), 97–109. https://doi.org/10.1007/s11769-017-0849-y.

Feng, W., et al., 2014. Oxygen isotope variations in rainfall, drip-water and speleothem calcite from a well-ventilated cave in Texas, USA: assessing a new speleothem temperature proxy. Geochim. Cosmochim. Acta 127, 233–250. https://doi.org/10.1016/j.gca.2013.11.039.

Fleitmann, D., et al., 2004. Palaeoclimatic interpretation of high-resolution oxygen isotope profiles derived from annually laminated speleothems from Southern Oman. Quat. Sci. Rev. 23 (7–8), 935–945. https://doi.org/10.1016/j.quascirev.2003.06.019.

Genty, D., et al., 2014. Rainfall and cave water isotopic relationships in two South-France sites. Geochim. Cosmochim. Acta 131, 323–343. https://doi.org/10.1016/j.gca.2014.01.043.

Gourcy, L.L. et al., 2005. Stable oxygen and hydrogen isotopes in precipitation. Isotopes in the Water Cycle: Past, Present and Future of a Developing Science. Springer, pp. 39–51. DOI:10.1007/1-4020-3023-1_4.

Hendy, C.H., 1971. The isotopic geochemistry of speleothems—I. The calculation of the effects of different modes of formation on the isotopic composition of speleothems and their applicability as palaeoclimatic indicators. Geochim. Cosmochim. Acta 35 (8), 801–824.

Hoffmann, G., Heimann, M., 1997. Water isotope modeling in the Asian monsoon region. Quat. Int. 37 (2), 115–128. https://doi.org/10.1016/1040-6182(96)00004-3.

Hu, C., et al., 2008. Quantification of Holocene Asian monsoon rainfall from spatially separated cave records. Earth Planet. Sci. Lett. 266 (3–4), 221–232. https://doi.org/10.1016/j.epsl.2007.10.015.

IAEA/WMO, 2001. Global Network of Isotopes in Precipitation. The GNIP Database. Available from: http://isohis.iaea.org.

Ishizaki, Y., et al., 2012. Interannual variability of (H2O)-O-18 in precipitation over the Asian monsoon region. J. Geophys. Res. 117. https://doi.org/10.1029/2011jd015890.

Johnson, K.R., Ingram, B.L., 2004. Spatial and temporal variability in the stable isotope systematics of modern precipitation in China: implications for paleoclimate reconstructions. Earth Planet. Sci. Lett. 220 (3–4), 365–377. https://doi.org/10.1016/s0012-821x(04)00036-6.

Jones, I.C., Banner, J.L., 2003. Estimating recharge thresholds in tropical karst island aquifers: Barbados, Puerto Rico and Guam. J. Hydrol. 278 (1–4), 131–143. https://doi.org/10.1016/s0022-1694(03)00138-0.

Ju, J.H., Slingo, J., 1995. The Asian summer monsoon and ENSO. Q. J. R. Meteorolog. Soc. 121 (525), 1133–1168. https://doi.org/10.1002/qj.49712152509.

Kim, S.T., O'Neil, J.R., 1997. Equilibrium and nonequilibrium oxygen isotope effects in synthetic carbonates. Geochim. Cosmochim. Acta 61 (16), 3461–3475. https://doi.org/10.1016/s0016-7037(97)00169-5.

Lacelle, D., Lauriol, B., Clark, I.D., 2004. Seasonal isotopic imprint in moonmilk from Caverne de l'Ours (Quebec, Canada): implications for climatic reconstruction. Can. J. Earth Sci. 41 (12), 1411–1423. https://doi.org/10.1139/e04-080.

Lee, J.-E., Fung, I., 2008. “Amount effect” of water isotopes and quantitative analysis of post-condensation processes. Hydrol. Process. 22 (1), 1–8. https://doi.org/10.1002/hyp.6637.

Li, B., et al., 2000. Oxygen and carbon isotopic characteristics of rainwater, drip water and present speleothems in a cave in Guilin area, and their environmental meanings. Sci. China (Ser. D) 43 (03), 277–285.

Li, T.-Y., et al., 2011. Oxygen and carbon isotopic systematics of aragonite speleothems and water in Furong Cave, Chongqing, China. Geochim. Cosmochim. Acta 75 (15), 4140–4156. https://doi.org/10.1016/j.gca.2011.04.003.

Liang, Z.R., et al., 2013. Application of HYSPLIT model in definition of the onset of South China sea summer monsoon. J. Trop. Meteorol. 19 (2), 130–137.

Liu, J., et al., 2015. Holocene East Asian summer monsoon records in northern China and their inconsistency with Chinese stalagmite delta O-18 records. Earth Sci. Rev. 148, 194–208. https://doi.org/10.1016/j.earscirev.2015.06.004.

Liu, J., et al., 2014. Stable isotopic compositions of precipitation in China. Tellus Ser. B 66 (1), 39–44. https://doi.org/10.3402/tellusb.v66.22567.

Luo, W., Wang, S., 2008. Transmission of oxygen isotope signals of precipitation-soil water-drip water and its implications in Liangfeng Cave of Guizhou, China. Chin. Sci. Bull. 53 (21), 3364–3370. https://doi.org/10.1007/s11434-008-0411-5.

Luo, W., Wang, S., Xie, X., 2013. A comparative study on the stable isotopes from precipitation to speleothem in four caves of Guizhou, China. Chem. Erde – Geochemistry 73 (2), 205–215. https://doi.org/10.1016/j.chemer.2012.05.002.

Luo, W., et al., 2014. Daily response of drip water isotopes to precipitation in Liangfeng Cave, Guizhou Province, SW China. Quat. Int. 349, 153–158. https://doi.org/10.1016/j.quaint.2014.01.043.

Ma, J., Gao, X., 2006. The Transportation Paths of Water Vapor and Its Relation to Climate Change over North China(in Chinese with English abstract). Plateau Meteorol. 25 (5), 893–899.

Maher, B.A., 2008. Holocene variability of the East Asian summer monsoon from Chinese cave records: a re-assessment. Holocene 18 (6), 861–866. https://doi.org/10.1177/0959683608095569.

Maher, B.A., Thompson, R., 2012. Oxygen isotopes from Chinese caves: records not of monsoon rainfall but of circulation regime. J. Quat. Sci. 27 (6), 615–624.

Mangini, A., Spötl, C., Verdes, P., 2005. Reconstruction of temperature in the Central Alps during the past 2000 yr from a δ18O stalagmite record. Earth Planet. Sci. Lett. 235 (3–4), 741–751. https://doi.org/10.1016/j.epsl.2005.05.010.

McDermott, F., et al., 2011. A first evaluation of the spatial gradients in delta O-18 recorded by European Holocene speleothems. Global Planet. Change 79 (3–4), 275–287. https://doi.org/10.1016/j.gloplacha.2011.01.005.

McDermott, F., et al., 1999. Holocene climate variability in Europe: Evidence from δ 18 O, textural and extension-rate variations in three speleothems. Quat. Sci. Rev. 18 (8), 1021–1038.

Merlivat, L., Jouzel, J., 1979. Global climatic interpretation of the deuterium-oxygen 18 relationship for precipitation. J. Geophys. Res. 84 (C8), 5029–5033. https://doi.org/10.1029/JC084iC08p05029.

Mickler, P.J., et al., 2004. Stable isotope variations in modern tropical speleothems: evaluating equilibrium vs. kinetic isotope effects. Geochim. Cosmochim. Acta 68 (21), 4381–4393. https://doi.org/10.1016/j.gca.2004.02.012.

Mischel, S.A., Scholz, D., Spotl, C., 2015. delta O-18 values of cave drip water: a promising proxy for the reconstruction of the North Atlantic Oscillation? Clim. Dyn. 45 (11–12), 3035–3050. https://doi.org/10.1007/s00382-015-2521-5.

Moerman, J.W., et al., 2014. Transformation of ENSO-related rainwater to dripwater delta O-18 variability by vadose water mixing. Geophys. Res. Lett. 41 (22), 7907–7915. https://doi.org/10.1002/2014gl061696.

Moore, M., Kuang, Z., Blossey, P.N., 2014. A moisture budget perspective of the amount effect. Geophys. Res. Lett. 41 (4), 1329–1335. https://doi.org/10.1002/2013gl058302.

O'Neil, J.R., Clayton, R.N., Mayeda, T.K., 1969. Oxygen isotope fractionation in divalent metal carbonates. J. Chem. Phys. 51 (12), 5547–5558. https://doi.org/10.1063/1.1671982.

Pape, J.R., et al., 2010. Controls on oxygen isotope variability in precipitation and cave drip waters, central Texas, USA. J. Hydrol. 385 (1–4), 203–215. https://doi.org/10.1016/j.jhydrol.2010.02.021.

Price, R.M., Swart, P.K., Willoughby, H.E., 2008. Seasonal and spatial variation in the stable isotopic composition (delta(18) O and delta D) of precipitation in south Florida. J. Hydrol. 358 (3–4), 193–205. https://doi.org/10.1016/j.jhydrol.2008.06.003.

Rozanski, K., Araguasaraguas, L., Gonfiantini, R., 1992. Relation between long-term trends of oxygen-18 isotope composition of precipitation and climate. Science 258 (5084), 981–985. https://doi.org/10.1126/science.258.5084.981.

Ruan, J., Hu, C., 2010. Seasonal variations and environmental controls on stalagmite calcite crystal growth in Heshang Cave, central China. Chin. Sci. Bull. 55 (34), 3929–3935. https://doi.org/10.1007/s11434-010-4193-1.

Shen, L., et al., 2010. The regional variabilities of the summer rainfall in Chinaand its relation with anomalous moisture transport during the recent 50 years(in Chinese with English abstract). Acta Meteorol. Sin. 68 (6), 918–931.

Shopov, Y., et al., 2004. Influence of solar luminosity over geomagnetic and climatic cycles as derived from speleothems. Int. J. Speleol. 33 (1/4), 19–24.

Song, C., et al., 2009. The constraints of strain partitioning and geochronology in Luonan-Luanchuan tectonic belts on Qinling orogenic belt. Sci. China Ser. D Earth Sci. 52 (3), 300–312. https://doi.org/10.1007/s11430-009-0021-3.

Stein, A.F., et al., 2015. NOAA's HYSPLIT Atmospheric Transport and Dispersion Modeling System. Bull. Am. Meteorol. Soc. 96 (12), 2059–2077. https://doi.org/10.1175/bams-d-14-00110.1.

Sun, Z., et al., 2017. Study on the Influence Factors of Modern Speleothem Hiatus: A case from Jiguan Cave, Henan (in Chinese with English abstract). Acta Sedimentol. Sin. 35 (1), 93–101.

Tan, L., et al., 2015. A Chinese cave links climate change, social impacts, and human adaptation over the last 500 years. Sci. Rep. 5 (4). https://doi.org/10.1038/srep12284.

Tan, M., 2014. Circulation effect: response of precipitation delta O-18 to the ENSO cycle in monsoon regions of China. Clim. Dyn. 42 (3–4), 1067–1077. https://doi.org/10.1007/s00382-013-1732-x.

Tan, M., 2016. Circulation background of climate patterns in the past millennium: uncertainty analysis and re-reconstruction of ENSO-like state. Sci. China Earth Sci. 59 (6), 1225–1241.

Thomas, E.K., et al., 2016. Heterodynes dominate precipitation isotopes in the East Asian monsoon region, reflecting interaction of multiple climate factors. Earth Planet. Sci. Lett. 455, 196–206. https://doi.org/10.1016/j.epsl.2016.09.044.

Tooth, A.F., Fairchild, I.J., 2003. Soil and karst aquifer hydrological controls on the geochemical evolution of speleothem-forming drip waters, Crag Cave, southwest Ireland. J. Hydrol. 273 (1–4), 51–68. https://doi.org/10.1016/s0022-1694(02)00349-9.

Treble, P.C., et al., 2005. In situ measurement of seasonal delta O-18 variations and analysis of isotopic trends in a modem speleothem from southwest Australia. Earth Planet. Sci. Lett. 233 (1–2), 17–32. https://doi.org/10.1016/j.epsl.2005.02.013.

Tremaine, D.M., Froelich, P.N., Wang, Y., 2011. Speleothem calcite farmed in situ: Modern calibration of delta O-18 and delta C-13 paleoclimate proxies in a continuously-monitored natural cave system. Geochim. Cosmochim. Acta 75 (17), 4929–4950. https://doi.org/10.1016/j.gca.2011.06.005.

Vaks, A., et al., 2003. Paleoclimate reconstruction based on the timing of speleothem growth and oxygen and carbon isotope composition in a cave located in the rain shadow in Israel. Quat. Res. 59 (2), 182–193. https://doi.org/10.1016/s0033-5894(03)00013-9.

Van Rampelbergh, M., et al., 2013. Mid- to late Holocene Indian Ocean Monsoon variability recorded in four speleothems from Socotra Island, Yemen. Quat. Sci. Rev. 65, 129–142. https://doi.org/10.1016/j.quascirev.2013.01.016.

Vuille, M., et al., 2005. Stable isotopes in precipitation in the Asian monsoon region. J. Geophys. Res. 110 (D23). https://doi.org/10.1029/2005jd006022.

Wang, B., LinHo, 2002. Rainy season of the Asian-Pacific summer monsoon. J. Clim. 15 (4), 386–398. https://doi.org/10.1175/1520-0442(2002)015<0386:rsotap>2.0.co;2.

Wang, X., et al., 2017. Hydroclimate changes across the Amazon lowlands over the past 45,000 years. Nature 541 (7636), 204–207. https://doi.org/10.1038/nature20787.

Wang, X., et al., 2015. Characteristics of atmospheric precipitation isotopes and isotopic evidence for the moisture origin in Yushugou River basin, Eastern Tianshan Mountains, China. Quat. Int. 380–381, 106–115. https://doi.org/10.1016/j.quaint.2014.12.023.

Wang, Y.J., et al., 2001. A high-resolution absolute-dated Late Pleistocene monsoon record from Hulu Cave, China. Science 294 (5550), 2345–2348. https://doi.org/10.1126/science.1064618.

Wang, Y.J., et al., 2005. The Holocene Asian monsoon: links to solar changes and North Atlantic climate. Science 308 (5723), 854–857. https://doi.org/10.1126/science.1106296.

Wei, K.Q., Lin, R.F., 1994. The influence of the monsoon climate on the isotopic composition of precipitation in China (in Chinese with English abstract). Geochimica 23 (1), 32–41.

Williams, P.W., Fowler, A., 2002. Relationship between oxygen isotopes in rainfall, cave percolation waters at Waitomo, New Zealand. J. Hydrol. NZ 41 (1), 53–70.

Xie, L., et al., 2011. Daily δ^{18}O and δD of precipitations from 2007 to 2009 in Guangzhou,

South China: Implications for changes of moisture sources. J. Hydrol. 400 (3–4), 477–489. https://doi.org/10.1016/j.jhydrol.2011.02.002.
Yang, H., et al., 2016. Interannual controls on oxygen isotope variability in Asian monsoon precipitation and implications for paleoclimate reconstructions. J. Geophys. Res. 121 (14), 8410–8428. https://doi.org/10.1002/2015jd024683.
Yonge, C.J., et al., 1985. Stable isotope studies of cave seepage water. Chem. Geol. 58 (1–2), 97–105. https://doi.org/10.1016/0009-2541(85)90182-2.
Yu, W., et al., 2014. Stable oxygen isotope differences between the areas to the north and south of Qinling Mountains in China reveal different moisture sources. Int. J. Climatol. 34 (6), 1760–1772. https://doi.org/10.1002/joc.3799.
Yuan, D.X., et al., 2004. Timing, duration, and transitions of the Last Interglacial Asian Monsoon. Science 304 (5670), 575–578. https://doi.org/10.1126/science.1091220.
Zheng, F., Zhu, J., 2015. Observed splitting eastbound propagation of subsurface warm water over the equatorial Pacific in early 2014. Science Bulletin 60 (4), 477–482. https://doi.org/10.1007/s11434-014-0678-7.
Zheng, S., Hou, F., Ni, B., 1983. The study of stable hydrogen and oxygen isotope in Chinese meteoric waters (in Chinese). Chin. Sci. Bull. 28 (13) 801-801.
Zhu, Z., et al., 2017. Holocene ENSO-related cyclic storms recorded by magnetic minerals in speleothems of central China. PNAS 114 (5), 852–857. https://doi.org/10.1073/pnas.1610930114.